Electronic Supplementary Material (ESI) for Inorganic Chemistry Frontiers
This journal is © The Partner Organisations 2014

Supplementary Data

Polymer-Based Biocompatible Fluorescent Sensor for Nano-molar Detection of Zn^{2+} in Aqueous Medium and Biological Samples

Kamalpreet Kaur[a], Manjot Kaur[b], Amanpreet Kaur[c], Jasminder Singh[b], Narinder Singh[a], Susheel K. Mittal[b,*], Navneet Kaur[c,*]

[a]Department of Chemistry, Indian Institute of Technology Ropar, Rupnagar, Punjab 140001, India

[b]School of Chemistry & Biochemistry, Thapar University, Patiala 147004, India

[c]Centre for Nanoscience & Nanotechnology, Panjab University, Chandigarh, Punjab 160014, India

List of Contents

This journal is © The Partner Organisations 2014

Figure S15. Fluorescence emission spectra of **2c**. Zn^{2+} complex (20 μM) upon successive addition of EDTA (0-40 μM) in HEPES buffered (10 mM, pH=7.0) DMF/H_2O (7:3, v/v) solvent system.

Figure S16. Showing the course of Fluorescence intensity at 418 nm with time (0-20 min) for 20 μM of **2c**. Zn^{2+} complex upon addition of 40 μM of EDTA in HEPES buffered (10 mM, pH=7.0) DMF/H_2O (7:3, v/v) solvent system.

Figure S17: Dose-response curve for **2c** for the calculation of IC_{50} value

Figure S18. Calibration curve for Zn^{2+} ion using electrode with ionophore **2a-c**.

Figure S19. Working pH range of electrodes with ionophore **2a-c**.

Figure S20. Potentiometric titration curves for electrodes with ionophore **2a-c**.

Table S1. Total energies of optimized keto and enol forms of receptors **2a**, **2b** and **2c**.

Table S2. Slopes of calibration curves for Zn (II) ions using electrodes with ionophores **2a-c**.

Table S3. Selectivity coefficients of Zn^{2+} ion selective electrodes for different interfering ions (1×10^{-3}M) by fixed interference method.

Table S4. A comparison of quantum yield of **2c**, **2c** after complexation with Zn^{2+}.

Table S5. A comparison of results obtained for spiked Zn^{2+} in water samples using proposed probe and AAS.

Scheme S1. Synthesis of monomer **3**.

Figure S21. Mass spectrum of **3**.

Figure S22. DFT calculated partial structures of receptor **2a-c**: (A) Enol and Keto forms of receptor **2a**; (B) Enol and Keto forms of receptor **2b**; (C) Enol and Keto forms of receptor **2c**; DFT calculations were performed at B3LYP/6-31G* level; red, blue and grey spheres refer to O, N and C atoms respectively).

Figure S23. (A) Changes in fluorescence intensity of receptor **2a** (10 μM) upon addition of 50 μM of a particular metal nitrate salts in HEPES buffered (10 mM, pH=7.0) DMF/H_2O (7:3, v/v); with λ_{ex} = 310 nm; (B) Influence of some metal ions on the Zn^{2+} based triggering of fluorescence intensity of **2a**.

Figure S24. (A) Changes in fluorescence intensity of receptor **2c** (10 μM) upon addition of 50 μM of a particular metal nitrate salts in HEPES buffered (10 mM, pH=7.0) DMF/H_2O (7:3, v/v); with λ_{ex} = 370 nm; (B) Selectivity of **2c** for Zn^{2+} compared to other metal ions: the presence of other metal ions has no effect for Zn^{2+} induced fluorescence intensity of **2c**.

Figure S25. Changes in fluorescence intensity of receptor **3** (10 μM) upon addition of 50 μM of a particular metal nitrate salts in HEPES buffered (10 mM, pH=7.0) DMF/H_2O (7:3, v/v); with λ_{ex} = 365 nm.

Figure S26. Changes in the Fluorescence spectra of **2c**.Zn^{2+} upon pH titration of a solution of **2c**.Zn^{2+} in DMF/H_2O (7:3, v/v) solvent system under: (A) acidic and (B) basic conditions.

This journal is © The Partner Organisations 2014

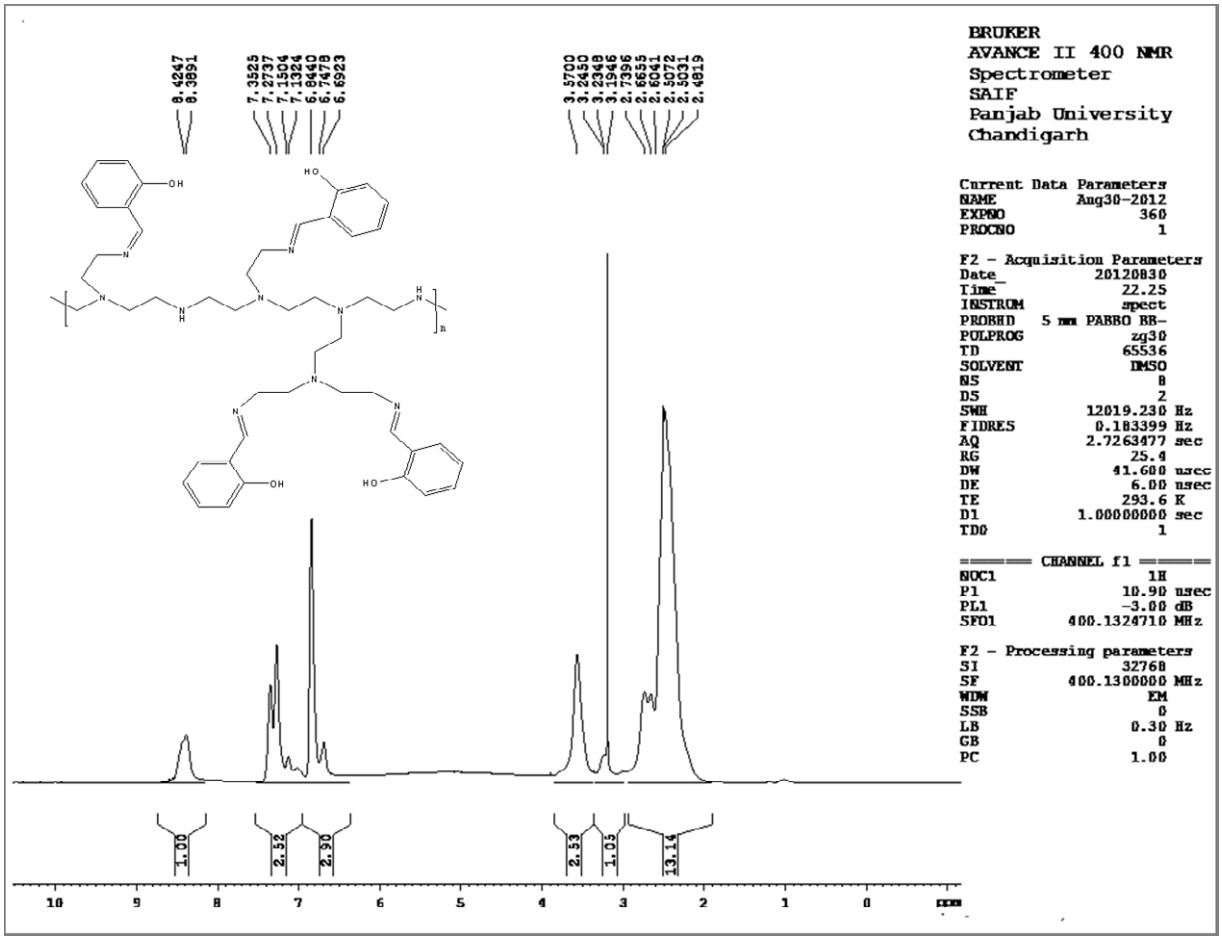

Figure S1. ^{1}H NMR spectrum of receptor **2a** in DMSO-d_6.

This journal is © The Partner Organisations 2014

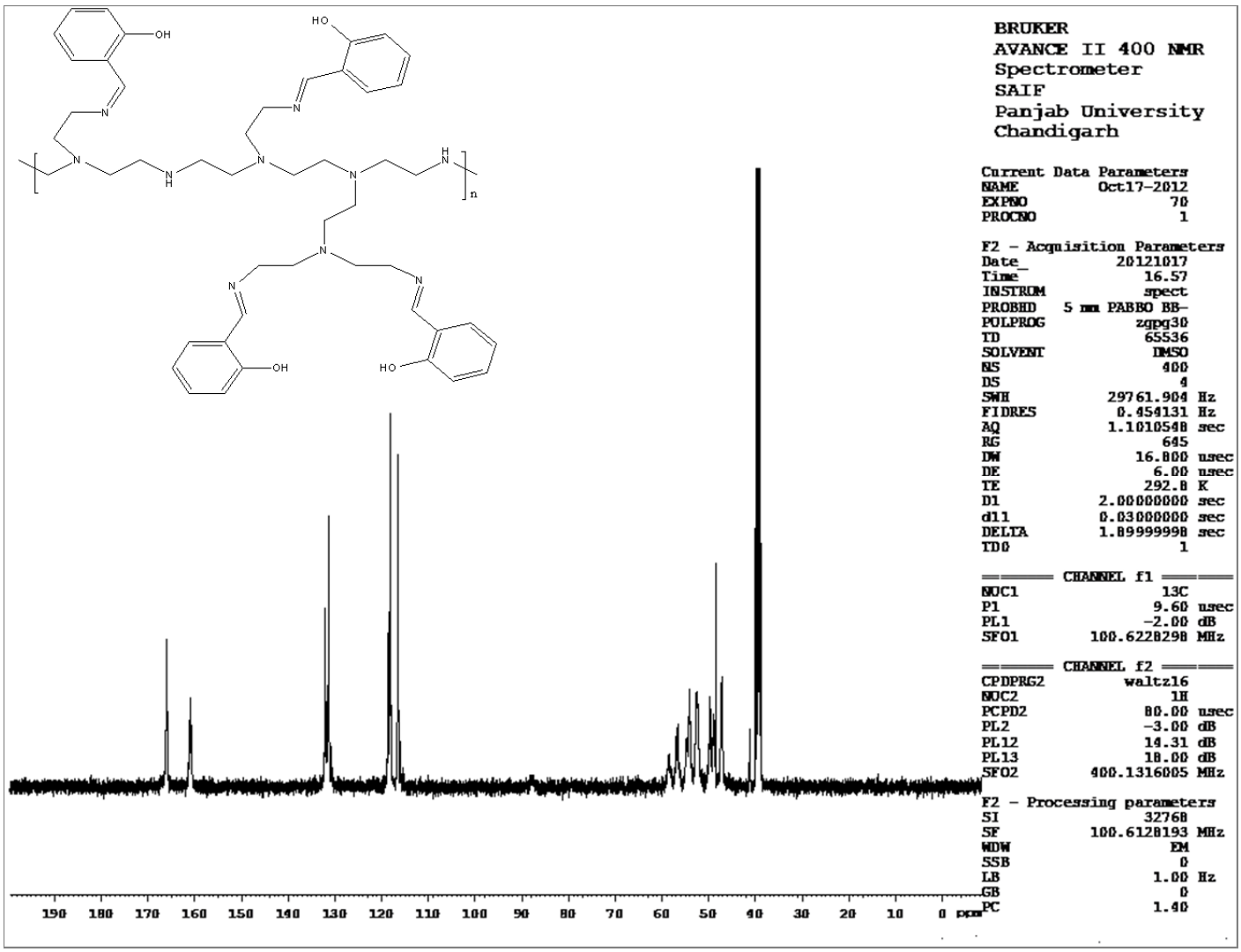

Figure S2 .^{13}C NMR spectrum of receptor **2a** in DMSO-d_6.

This journal is © The Partner Organisations 2014

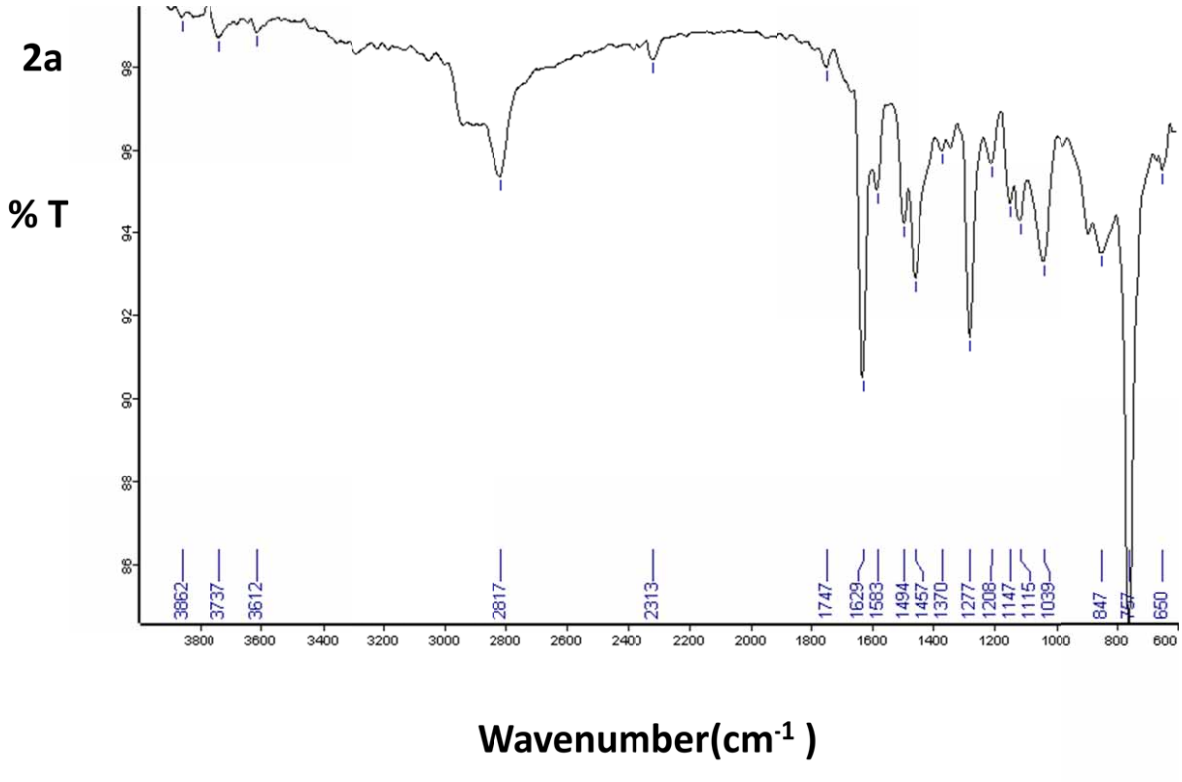

Figure S3. IR spectrum of receptor **2a.**

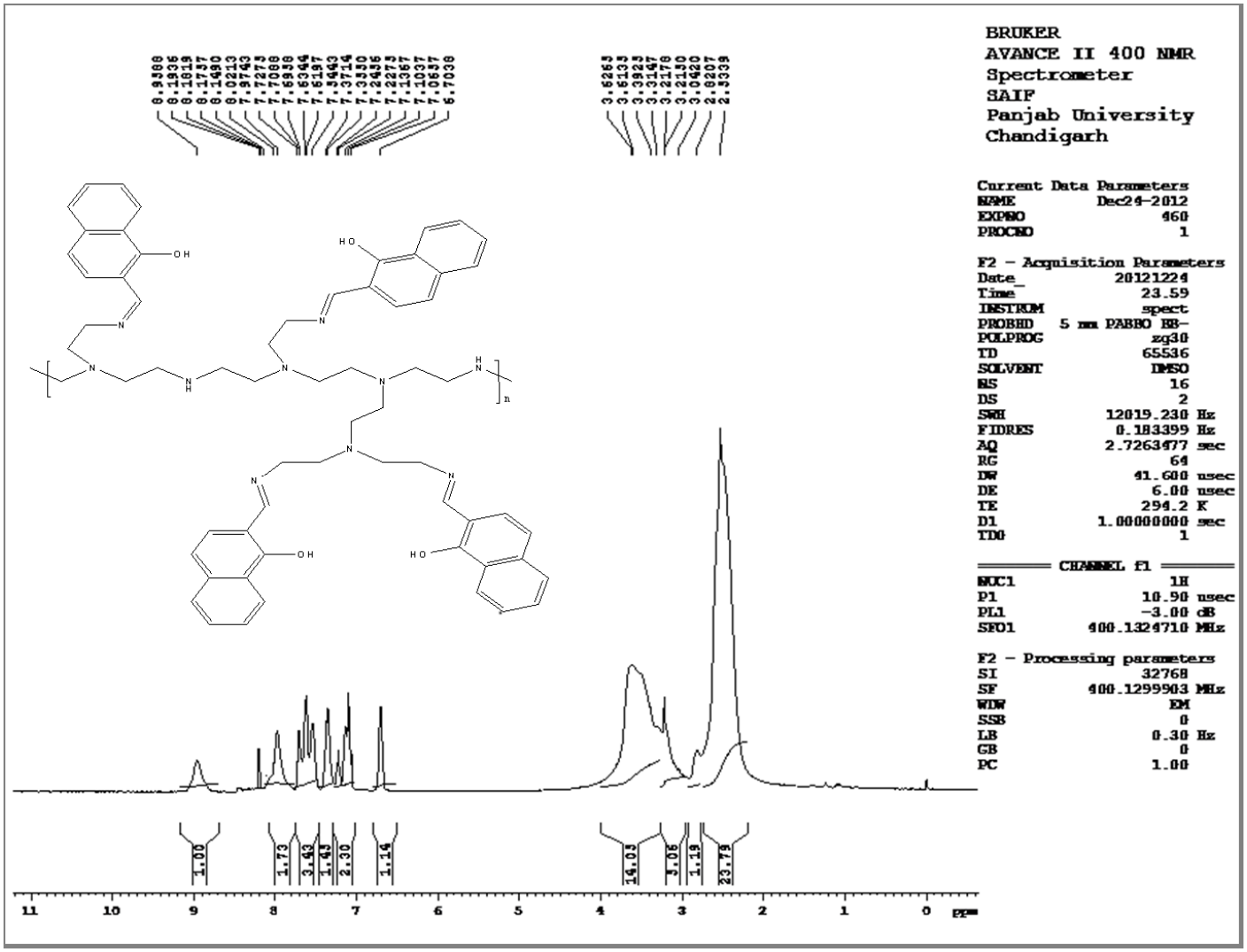

Figure S4. ^{1}H NMR spectrum of receptor **2b** in DMSO-d_6.

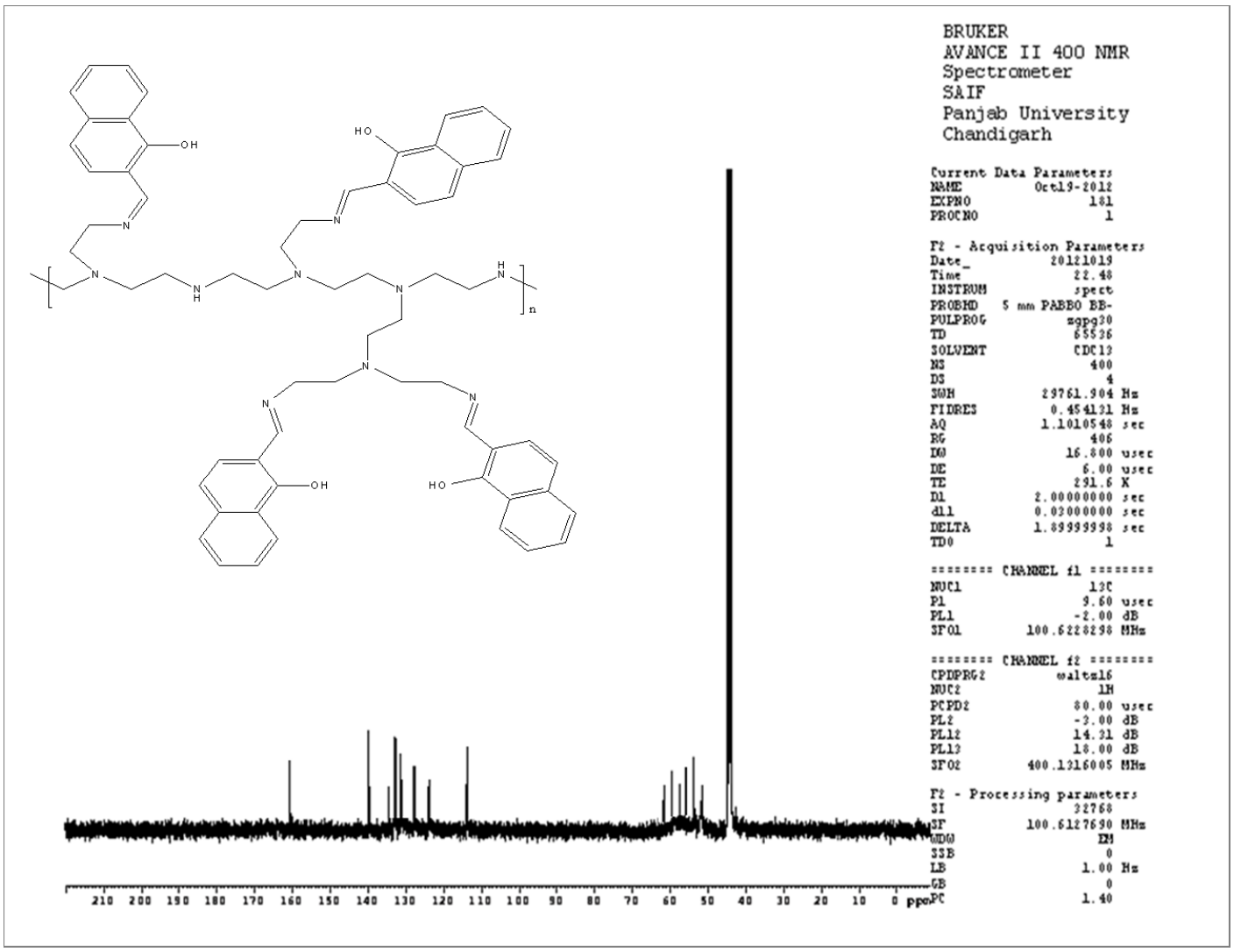

Figure S5. ^{13}C NMR spectrum of receptor **2b** in DMSO-d_6.

This journal is © The Partner Organisations 2014

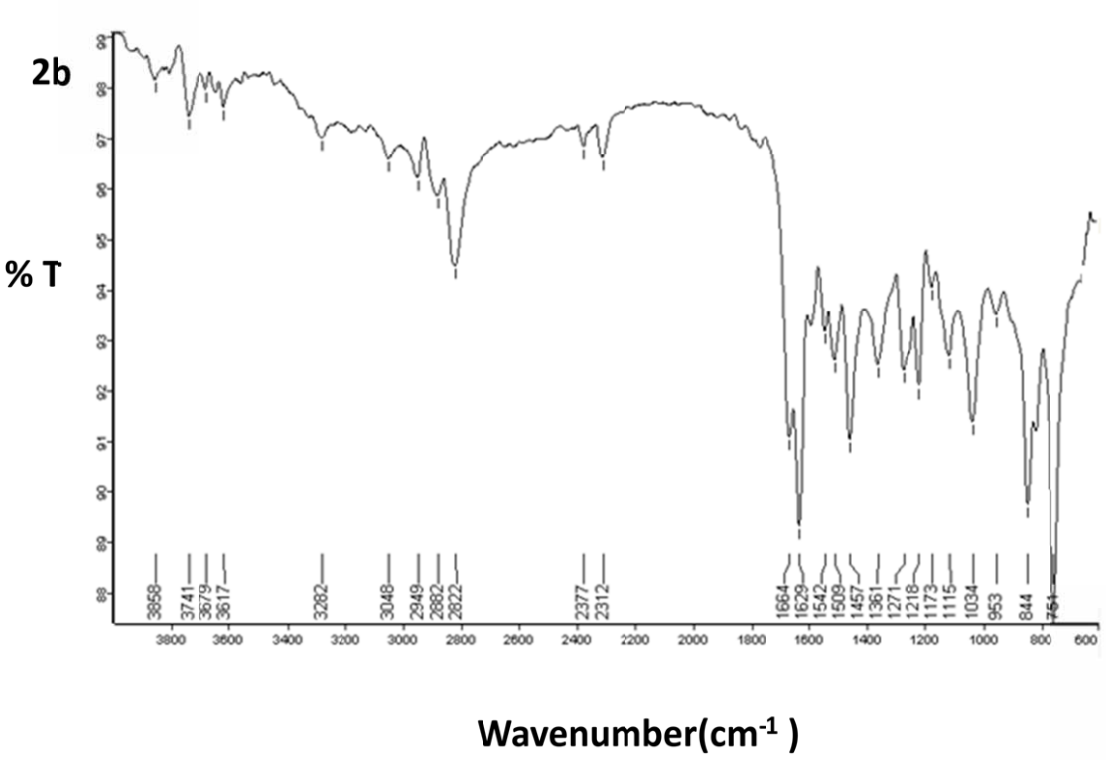

Figure S6. IR spectrum of receptor **2b.**

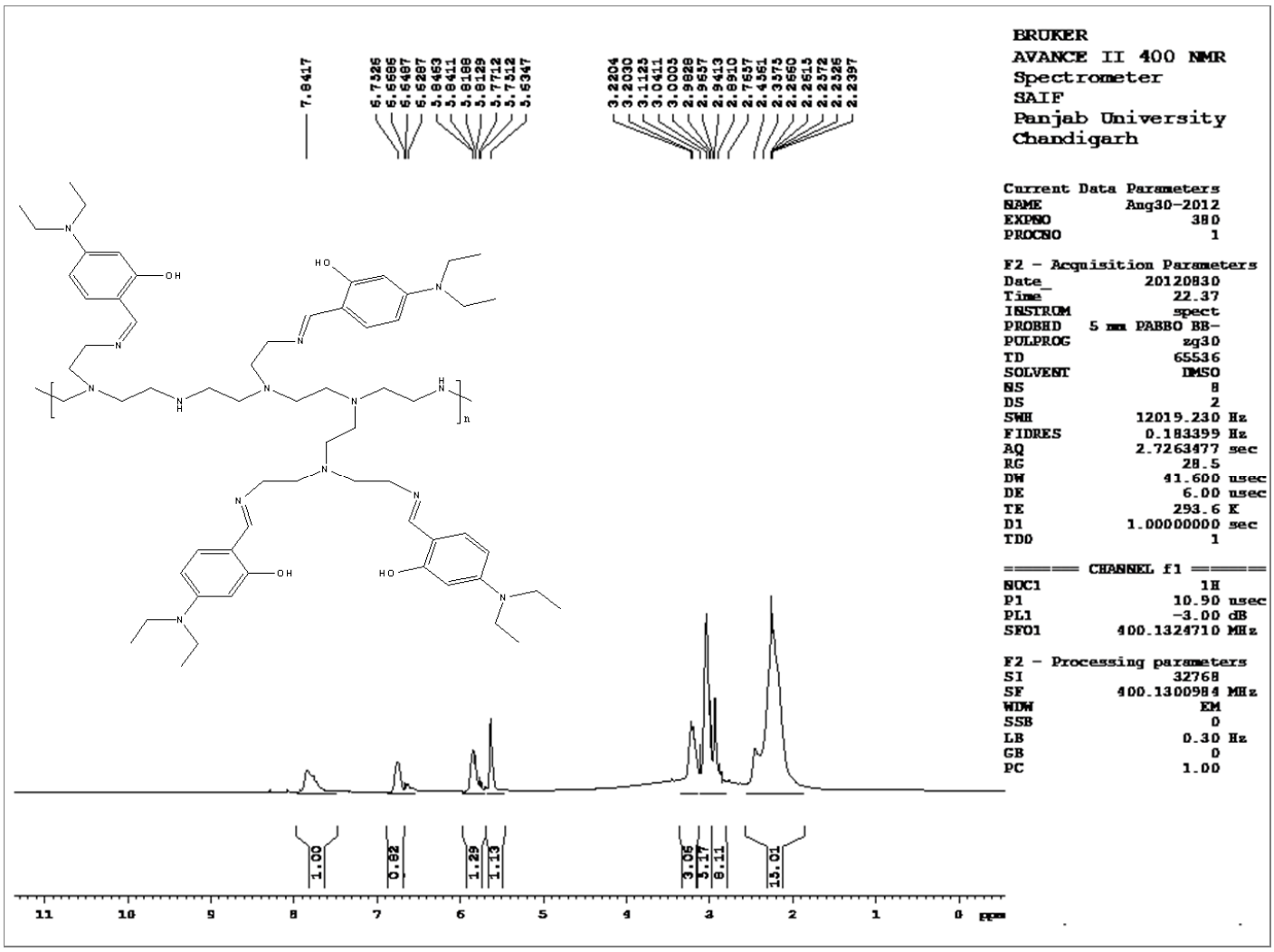

Figure S7. ^{1}H NMR spectrum of receptor **2c** in DMSO-d_6.

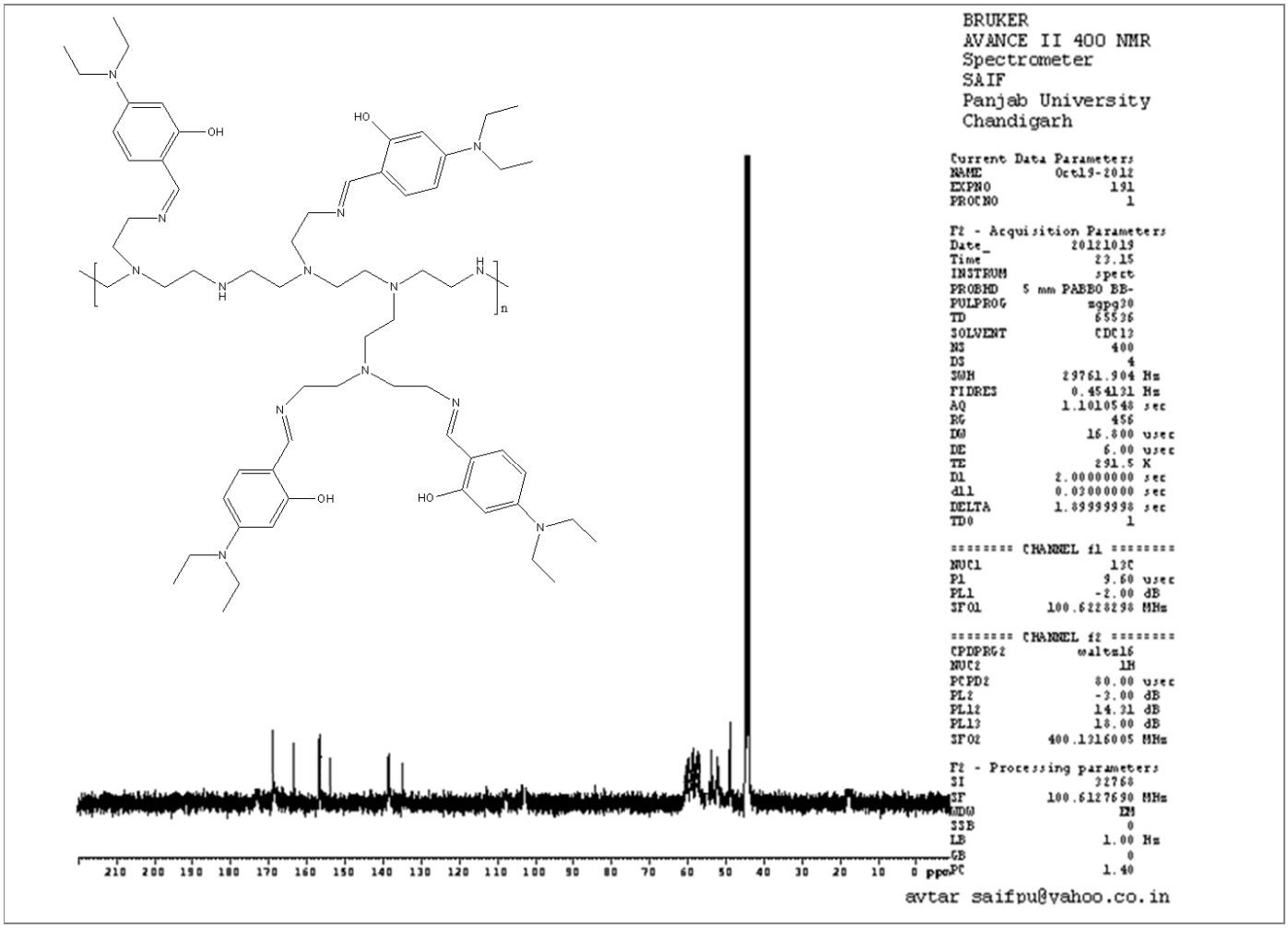

Figure S8. ^{13}C NMR spectrum of receptor **2c** in DMSO-d_6.

This journal is © The Partner Organisations 2014

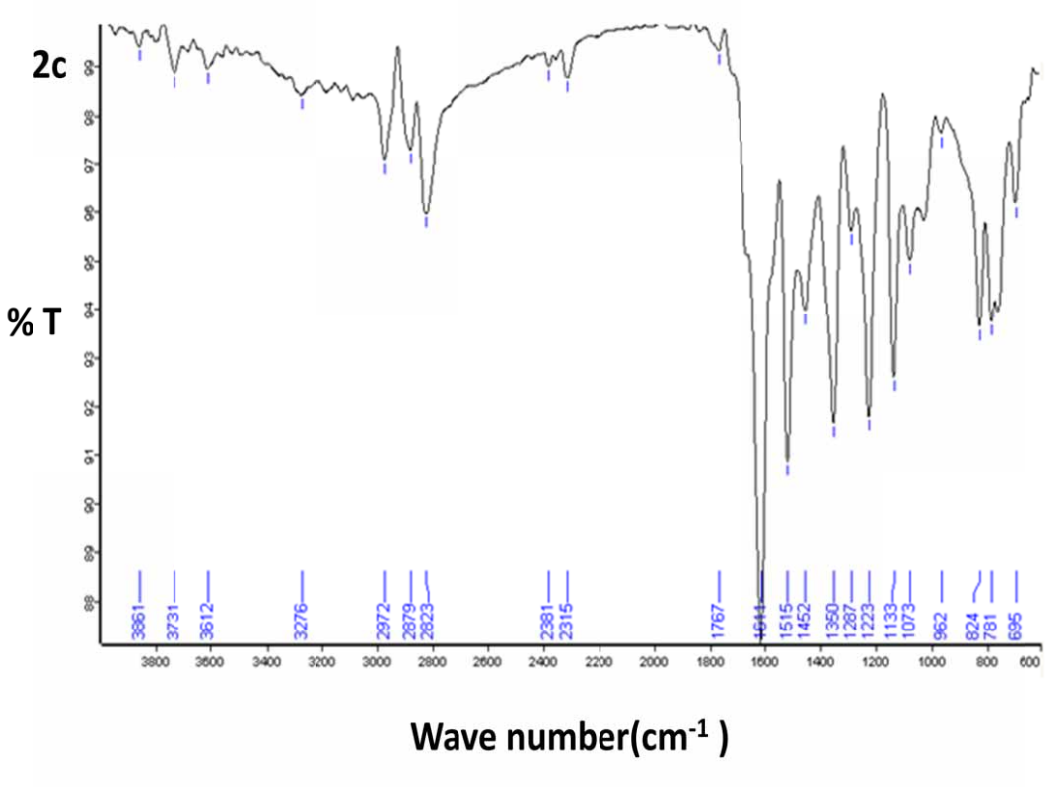

Figure S9. IR spectrum of receptor **2c.**

This journal is © The Partner Organisations 2014

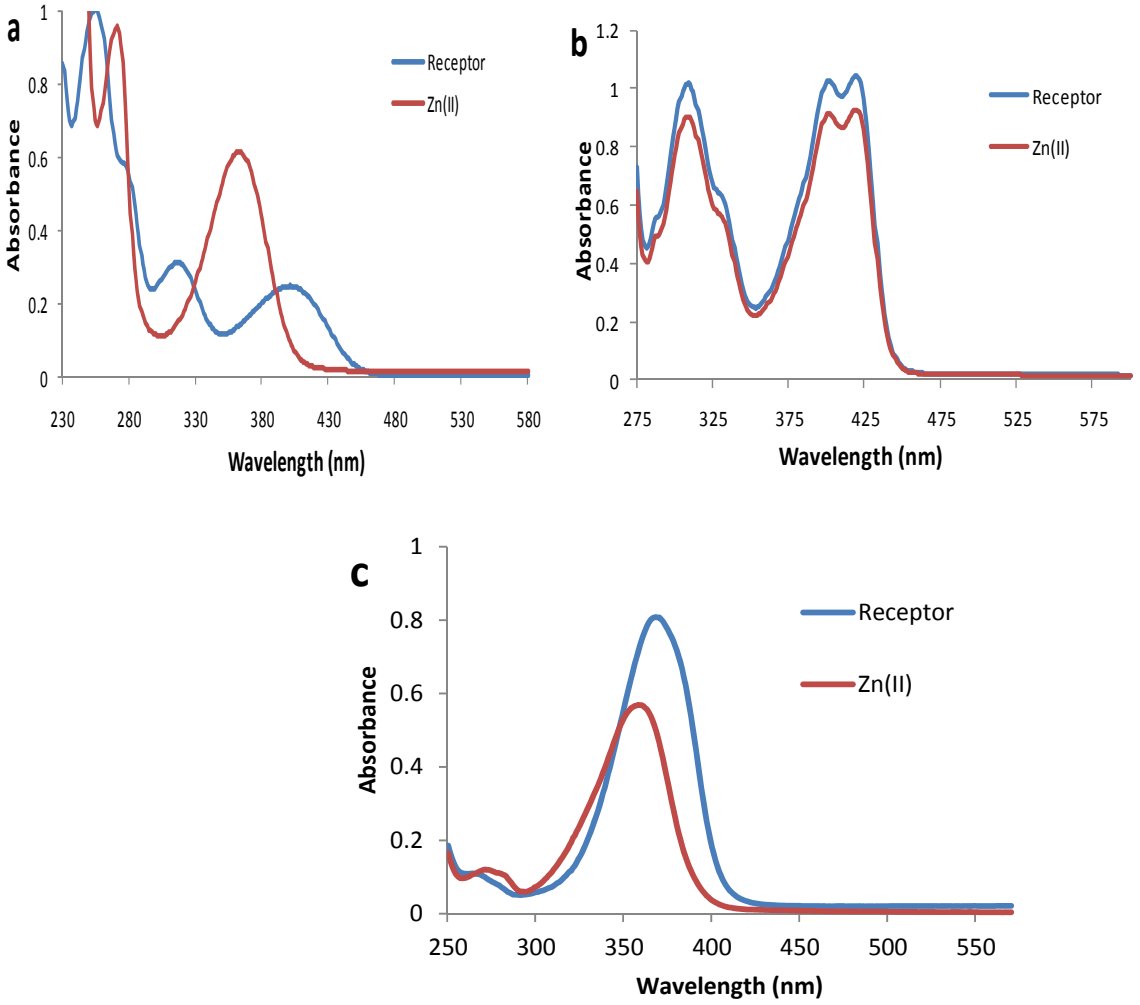

Figure S10. UV-Vis absorption spectra of (a) receptor **2a** (10 μM) upon addition of 50 μM of Zn^{2+} nitrate salt in HEPES buffered (10 mM, pH=7.0) DMF/H_2O (7:3, v/v) solvent system; (b) receptor **2b** (10 μM) upon addition of 50 μM of Zn^{2+} nitrate salt in HEPES buffered (10 mM, pH=7.0) DMF/H_2O (7:3, v/v) solvent system and (c) receptor **2c** (10 μM) upon addition of 50 μM of Zn^{2+} nitrate salt in HEPES buffered (10 mM, pH=7.0) DMF/H_2O (7:3, v/v) solvent system.

This journal is © The Partner Organisations 2014

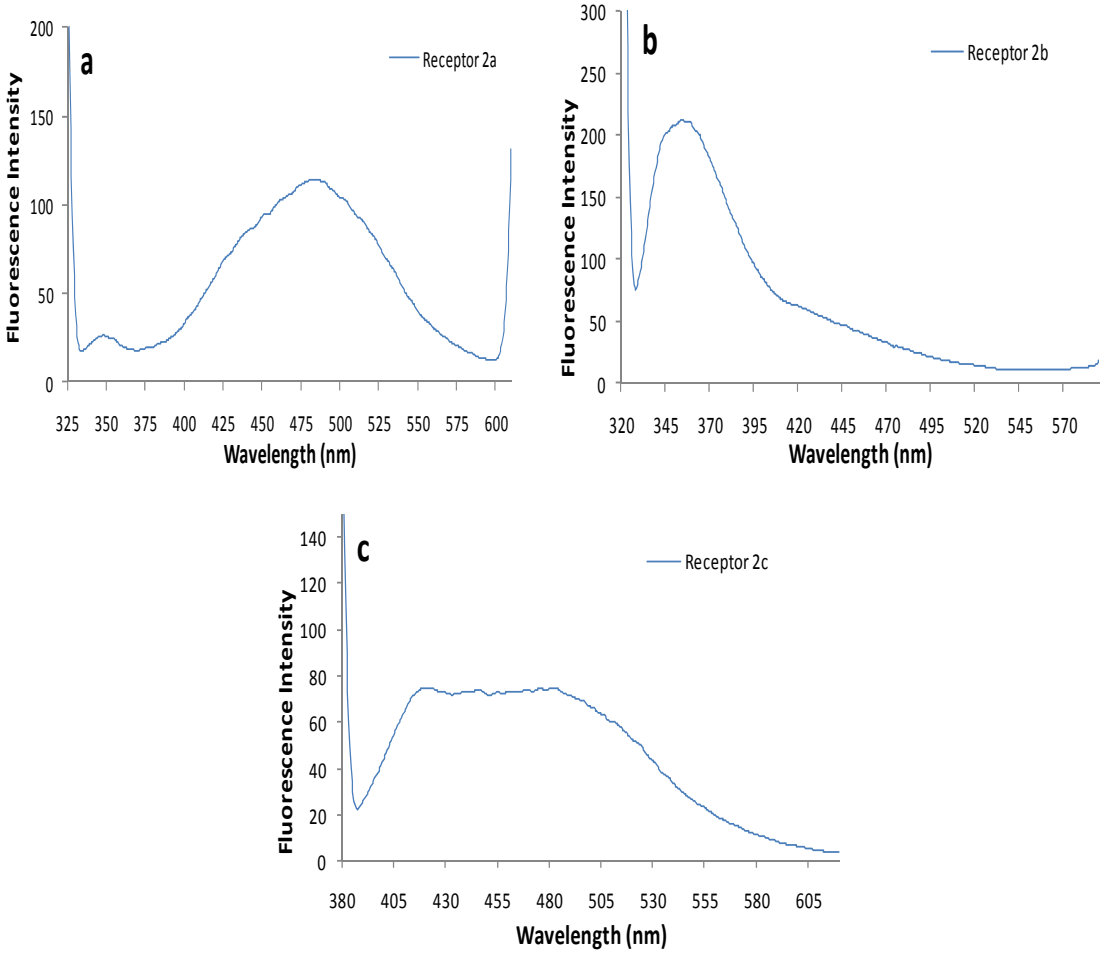

Figure S11. Fluorescence spectrum of (a) receptor **2a** (10 μM) recorded in HEPES buffered (10 mM, pH=7.0) DMF/H_2O (7:3, v/v) solvent system excited at 310 nm; (b) receptor **2b** (10 μM) recorded in HEPES buffered (10 mM, pH=7.0) DMF/H_2O (7:3, v/v) solvent system excited at 309 nm and (c) receptor **2c** (10 μM) recorded in HEPES buffered (10 mM, pH=7.0) DMF/H_2O (7:3, v/v) solvent system excited at 370 nm.

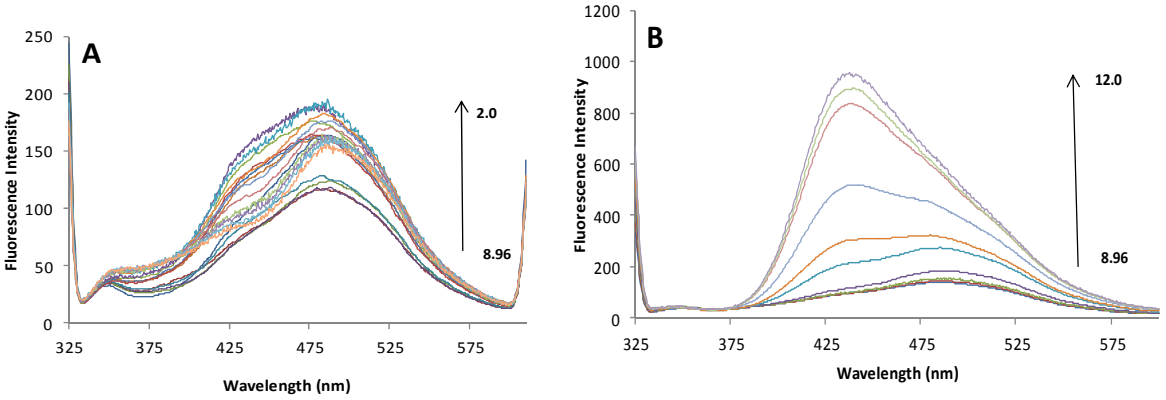

Figure S12. Changes in the Fluorescence spectra of **2a** upon pH titration of a solution of **2a** (10 μM) in DMF/H_2O (7:3, v/v) solvent system under**:** (**A**) acidic and (**B**) basic conditions.

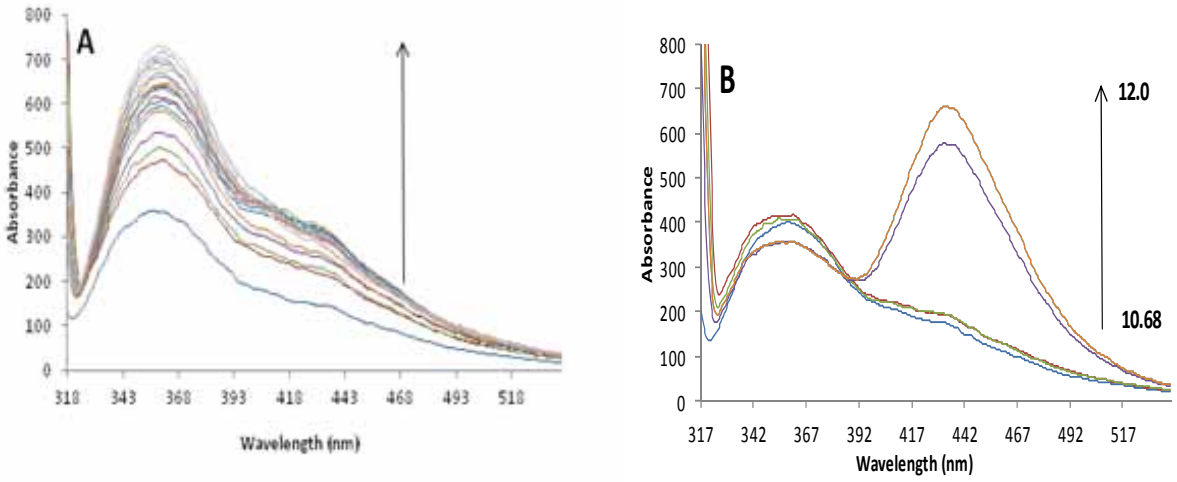

Figure S13. Changes in the Fluorescence spectra of **2b** upon pH titration of a solution of **2b** (15 μM) in DMF/H_2O (7:3, v/v) solvent system under**:** (**A**) acidic and (**B**) basic conditions.

This journal is © The Partner Organisations 2014

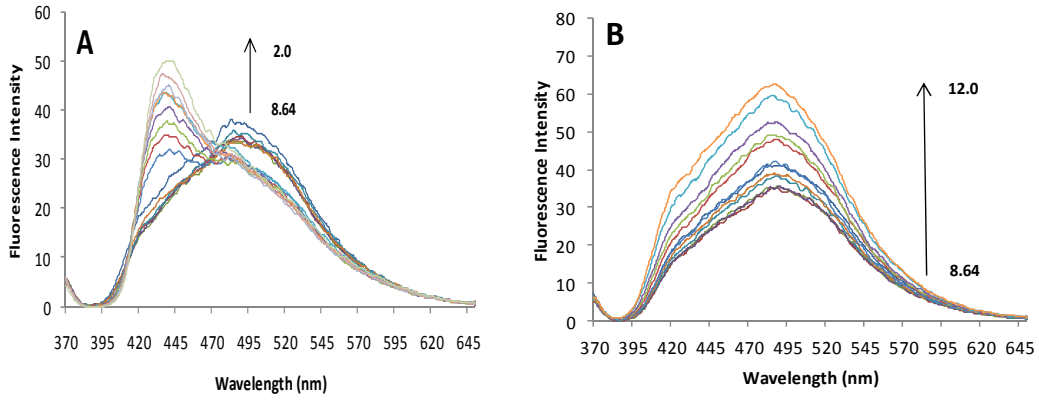

Figure S14. Changes in the Fluorescence spectra of **2c** upon pH titration of a solution of **2c** (8 μM) in DMF/H_2O (7:3, v/v) solvent system under**:** (**A**) acidic and (**B**) basic conditions.

Kinetic analysis of the recognition process and determination of activation energy

The first order binding process can be expressed using the following equation:

$$\ln[(A_\infty - A_t)/(A_\infty - A_o)] = kt$$

Where A_o,A_t and A_∞ are the fluorescence intensities of the host-guest complex at time 0, t and infinity respectively. *K* is the rate constant.

Under present investigations; for kinetic studies, the host guest reaction is progressing in the following way:

HOST	+	GUEST (*excess*)	→	Host-Guest Complex
2c.Zn^{2+} complex		EDTA		

In the above reaction changes in the Fluorescence emission intensity at 418 nm were monitored for the determination of *K*. The excess of EDTA was added to the solution of **2c**.Zn^{2+}; so that the reaction can be regarded as pseudo first order reaction i.e. kinetics depends only on the concentration of host.

This journal is © The Partner Organisations 2014

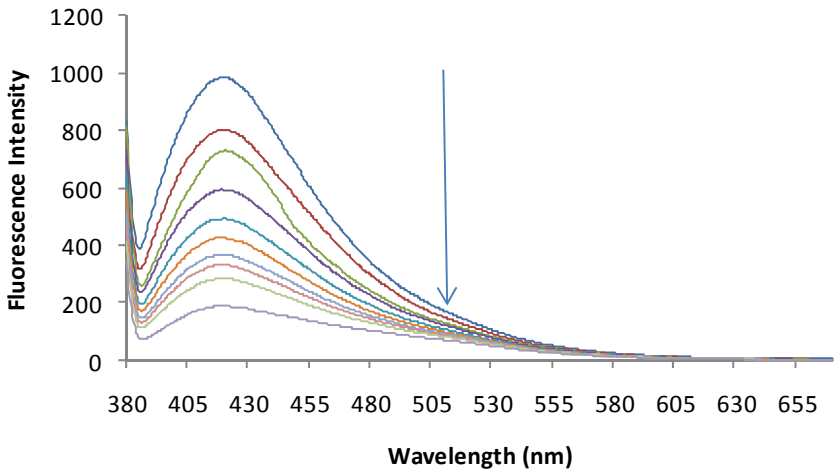

Figure S15: Fluorescence emission spectra of **2c**. Zn^{2+} complex (20 μM) upon successive addition of EDTA (0-40 μM) in HEPES buffered (10 mM, pH=7.0) DMF/H_2O (7:3, v/v) solvent system.

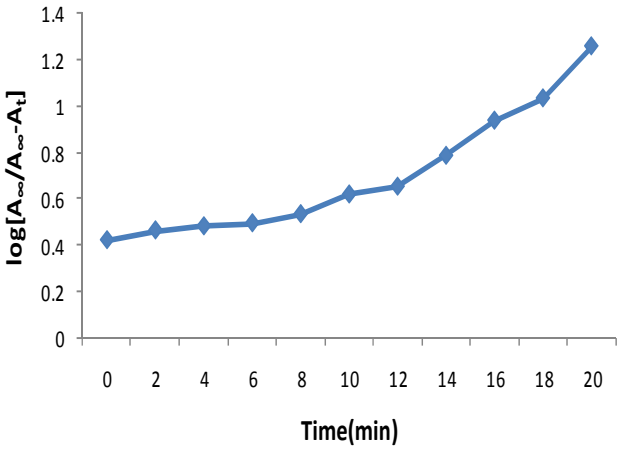

Figure S16: Showing the course of Fluorescence intensity at 418 nm with time (0-20 min) for 20 μM of **2c**. Zn^{2+} complex upon addition of 40 μM of EDTA in HEPES buffered (10 mM, pH=7.0) DMF/H_2O (7:3, v/v) solvent system.

This journal is © The Partner Organisations 2014

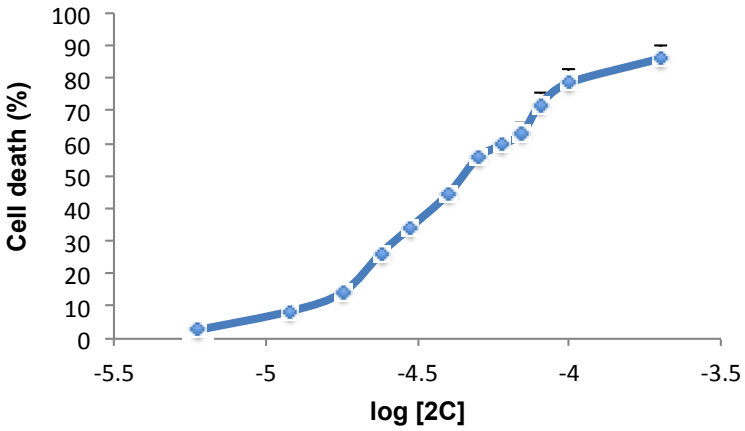

Figure S17: Dose-response curve for **2c** for the calculation of IC_{50} value

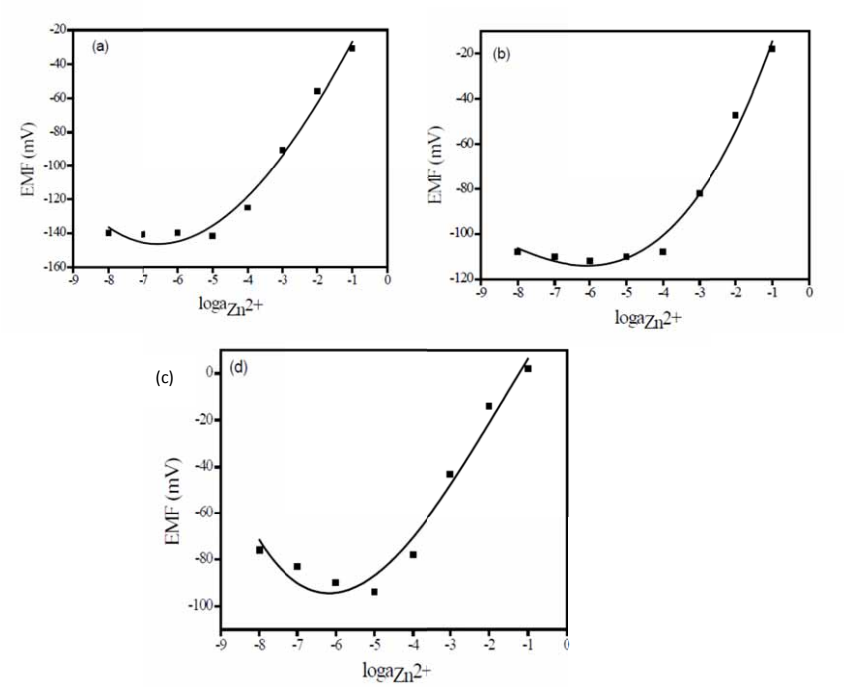

Figure S18: Calibration curve for Zn^{2+} ion using electrode with ionophore **2a-c**.

This journal is © The Partner Organisations 2014

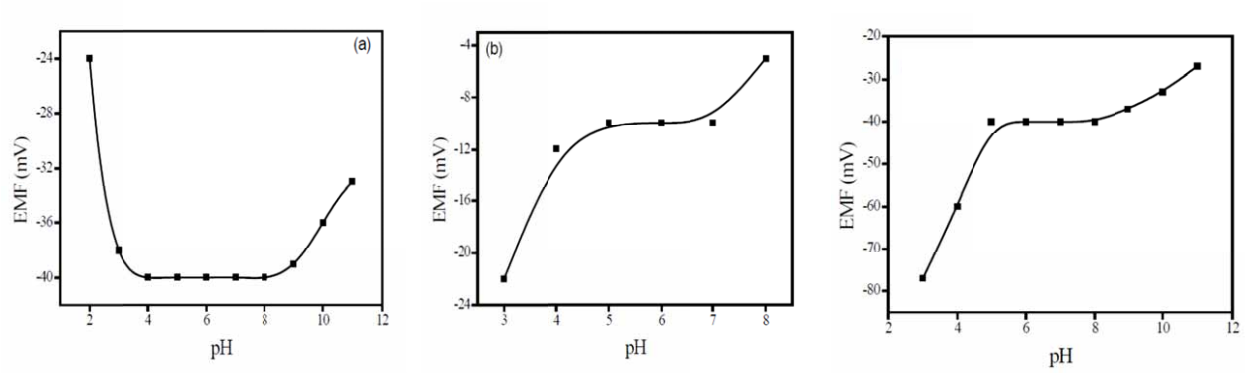

Figure S19: Working pH range of electrodes with ionophore **2a-c**.

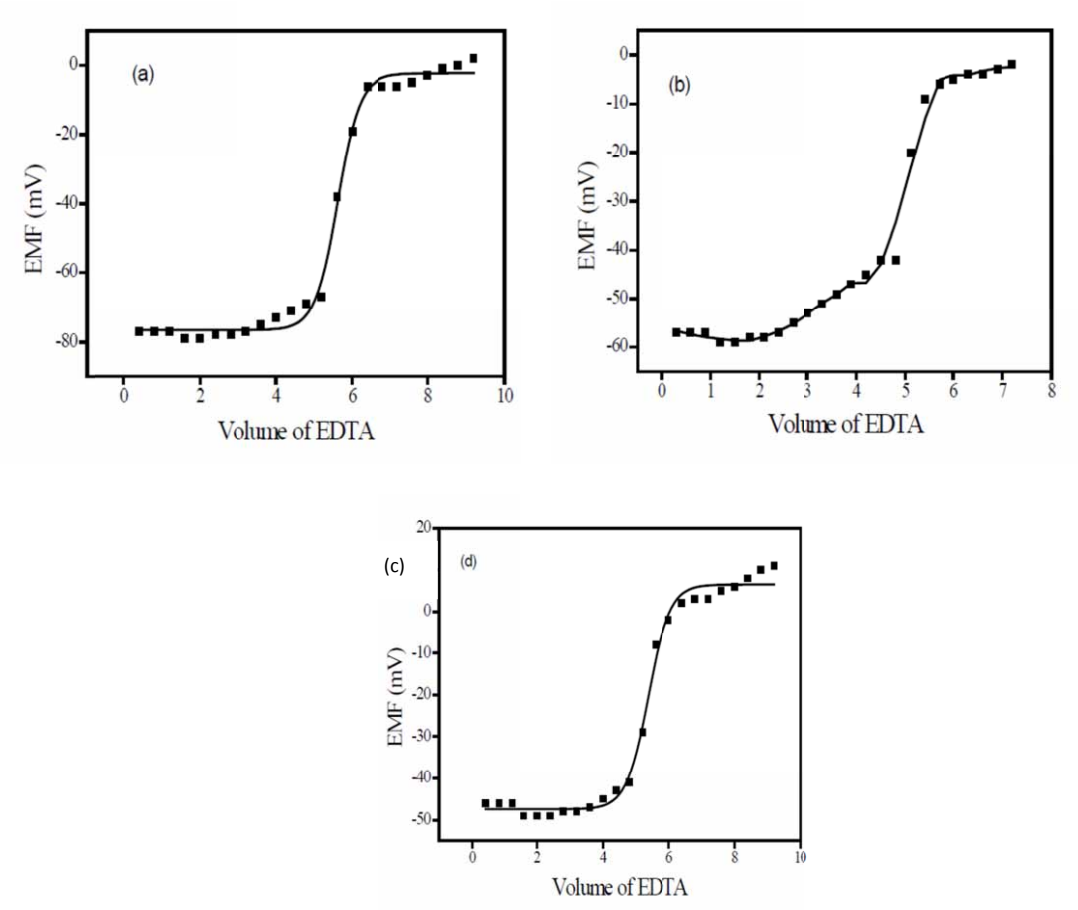

Figure S20: Potentiometric titration curves for electrodes with ionophore **2a-c**.

This journal is © The Partner Organisations 2014

Table S1. Total energies of optimized keto and enol forms of receptors **2a**, **2b** and **2c**

Tautomeric forms	Total energy (eV)
Receptor **2a** (Enol Form) Receptor **2a** (Keto Form)	-14102.943 -14105.392
Receptor **2b** (Enol Form) Receptor **2b** (Keto Form)	-18288.385 -18288.657
Receptor **2c** (Enol Form) Receptor **2c** (Keto Form)	-19897.040 -19897.857

Table S2. Slopes of calibration curves for Zn (II) ions using electrodes with ionophores **2a-c**.

S No.	Slope (mV/decade)		
	Ionophore, **2a**	Ionophore, **2b**	Ionophore, **2c**
1.	33	32	29
2.	30	30	27
3.	32	29	27
4.	33	30	27
Mean	32 ± 2.0	30.2 ± 1.5	27.5 ± 1.0

Table S3. Selectivity coefficients of Zn^{2+} ion selective electrodes for different interfering ions (1×10^{-3}M) by fixed interference method.

S. No.	**Interfering ions**	**Selectivity coefficient, log K**		
		2a	**2b**	**2c**
1.	Ca^{2+}	-1.0	-0.2	-0.5
2.	Mg^{2+}	0.0	0.4	-0.2
3.	Fe^{2+}	0.5	-	-
4.	Co^{2+}	-0.4	-0.3	-0.4
5.	Ni^{2+}	0.7	-0.3	-0.4
6.	Cu^{2+}	-0.4	-0.6	-0.5

This journal is © The Partner Organisations 2014

7.	Pb^{2+}	-1.3	-0.4	-1.1
8.	Cd^{2+}	-0.4	-0.4	-0.4

Table S4. A comparison of quantum yield of **2c**, **2c** after complexation with Zn^{2+}.

Sr. No.	**Polymer 2c**	**Polymer 2c + Zn^{2+}**
1	0.20	0.65
2	0.22	0.67
3	0.21	0.67
Mean	0.21±0.01	0.66±0.01

Fluorescence quantum yield[1] was determined using optically matching standard solutions at a particular excitation wavelength and quantum yield is calculated using the equation:

$$\Phi fs = \Phi fr \times \frac{1 - 10^{-ArLr}}{1 - 10^{-AsLs}} \times \frac{Ns^2}{Nr^2} \times \frac{Ds}{Dr}$$

Φfs and Φfr are the quantum yields of sample and the reference respectively, A_s and A_r are the absorbance of the sample and the reference respectively, Ds and Dr the respective areas of emission for sample and reference. Ls and Lr are the lengths of the absorption cells of sample and reference respectively. Ns and Nr are the refractive indices of the sample and reference solutions.

Table S5. A comparison of results obtained for spiked Zn^{2+} in water samples using proposed probe and AAS.

Sample Code	**Zn^{2+} (mg/mL) added**	**Polymer 2c (mean[a])**	**AAS (mean[a])**
Tap water 1	0.297	0.30	0.299
Tap water 2	1.485	1.49	1.48
Tap water 3	2.97	3.04	3.01
Tap water 4	5.94	5.96	5.97
Tap water 5	14.85	14.92	14.89

[a] Mean of three determinations.

To evaluate the real practical application of **2c**, the concentration of Zn^{2+} was analysed in the environmental water samples taken from tap. The initial AAS studies of sample showed the presence of less than 0.002 □g/mL content of Zn^{2+} in the water samples. Therefore, water samples spiked with Zn^{2+} were analysed for Zn^{2+} content using the **2c** in aqueous medium and AAS. The results show good agreement of spiked Zn^{2+} content observed and values determined by AAS. The results revealed that the present probe (**2c**) can work well in environmental samples.

This journal is © The Partner Organisations 2014

Scheme S1. Synthesis of monomer **3**.

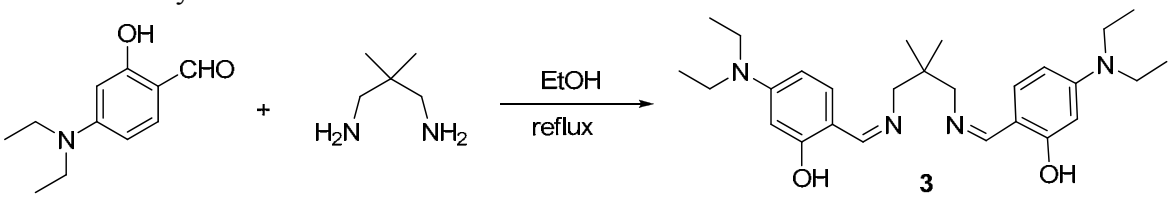

The monomer **3** was synthesized by adding 4-diethylamino-salicylaldehyde (2 mmol) to a solution of 3,3-dimethylpropylenediamine (1 mmol) in ethanol (10 ml). The mixture was refluxed for one hour. The monomer 3 precipitated as yellow solid which was filtered and washed with cold ethanol. % yield = 87%. ESI-MS (m/z) 475 (M+23); CHN analysis calcd. for ($C_{27}H_{40}N_4O_2$): C, 71.65; H, 8.91; N, 12.38; found: C, 71.68; H, 8.89; N, 12.41.

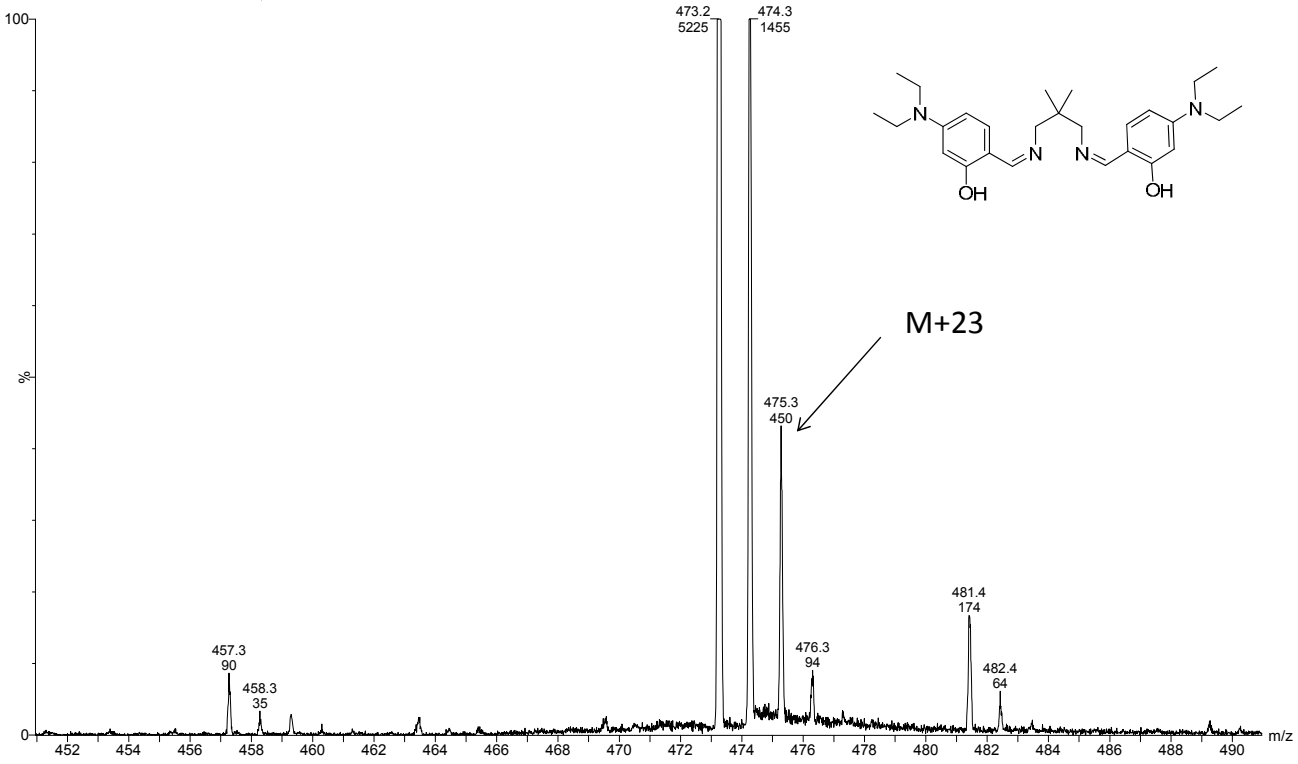

Figure S21. Mass spectrum of **3**.

This journal is © The Partner Organisations 2014

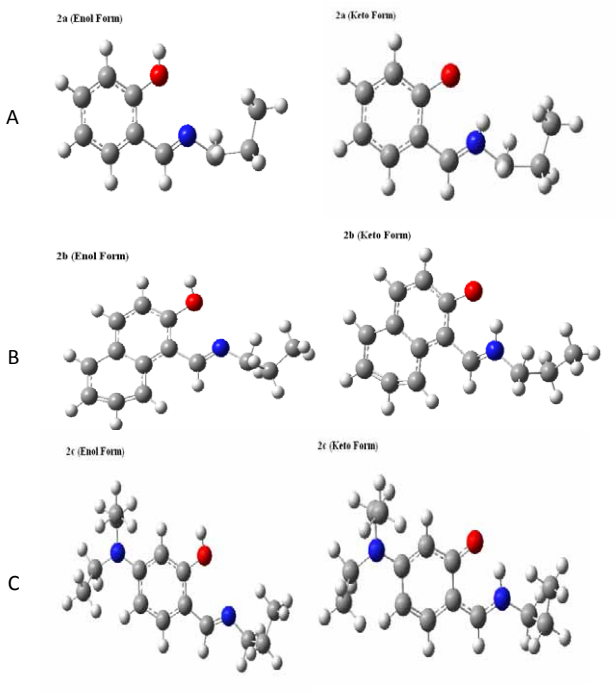

Figure S22. DFT calculated partial structures of receptor **2a-c**: (A) Enol and Keto forms of receptor **2a**; (B) Enol and Keto forms of receptor **2b**; (C) Enol and Keto forms of receptor **2c**; DFT calculations were performed at B3LYP/6-31G* level; red, blue and grey spheres refer to O, N and C atoms respectively).

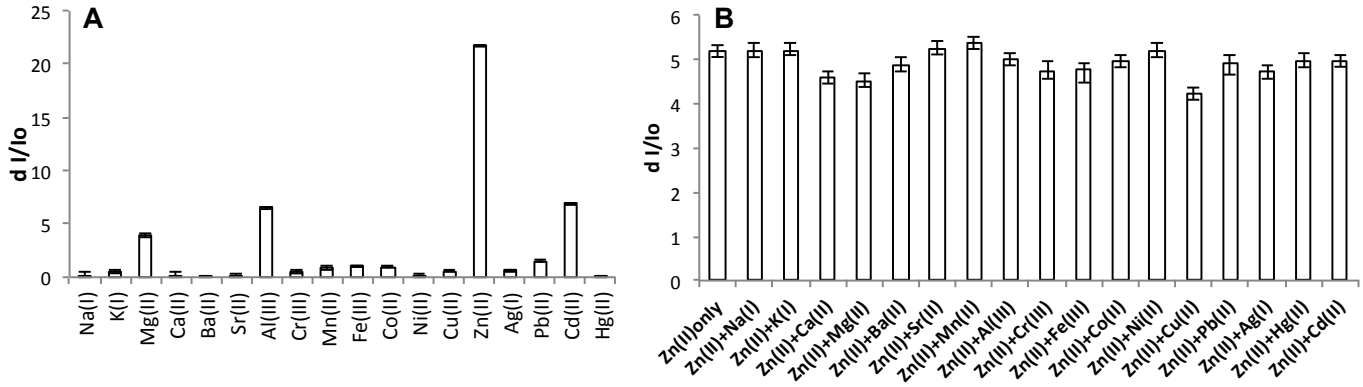

Figure S23. (A) Changes in fluorescence intensity of receptor **2a** (10 μM) upon addition of 50 μM of a particular metal nitrate salts in HEPES buffered (10 mM, pH=7.0) DMF/H_2O (7:3, v/v); with λ_{ex} = 310 nm; (B) Influence of some metal ions on the Zn^{2+} based triggering of fluorescence intensity of **2a**.

This journal is © The Partner Organisations 2014

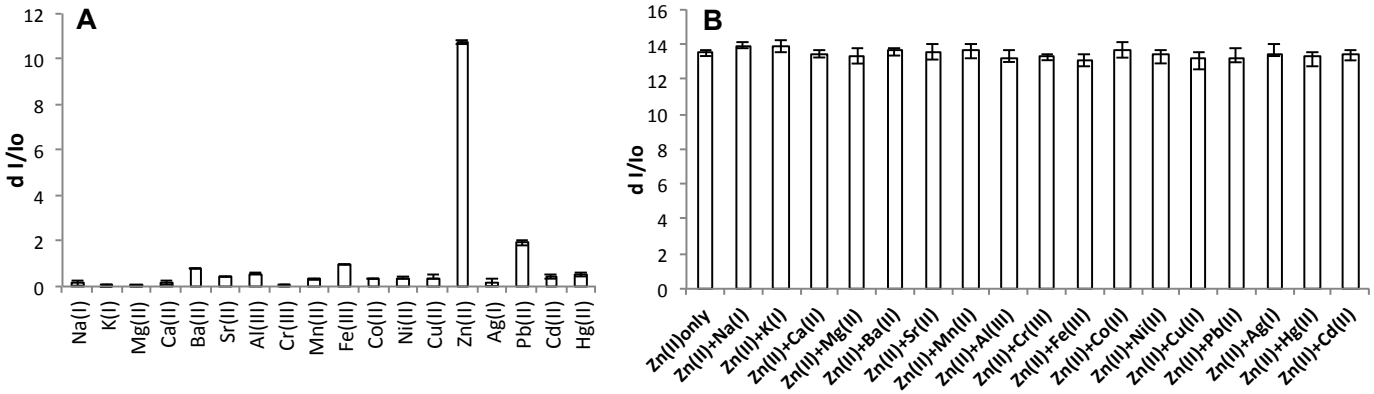

Figure S24. (A) Changes in fluorescence intensity of receptor **2c** (10 μM) upon addition of 50 μM of a particular metal nitrate salts in HEPES buffered (10 mM, pH=7.0) DMF/H_2O (7:3, v/v); with λ_{ex} = 370 nm; (B) Selectivity of **2c** for Zn^{2+} compared to other metal ions: the presence of other metal ions has no effect for Zn^{2+} induced fluorescence intensity of **2c**.

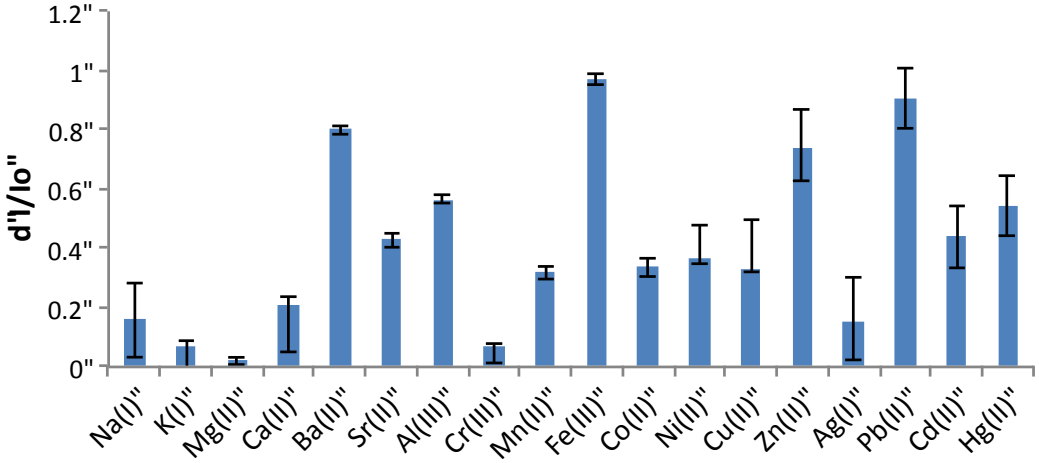

Figure S25. Changes in fluorescence intensity of receptor **3** (10 μM) upon addition of 50 μM of a particular metal nitrate salts in HEPES buffered (10 mM, pH=7.0) DMF/H_2O (7:3, v/v); with λ_{ex} = 365 nm.

This journal is © The Partner Organisations 2014

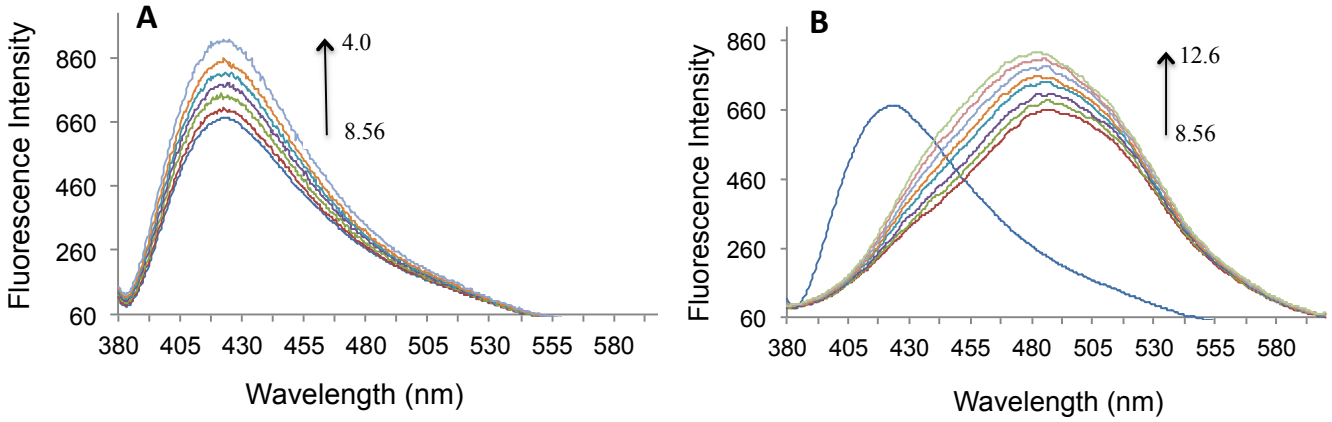

Figure S26. Changes in the Fluorescence spectra of **2c**.Zn^{2+} upon pH titration of a solution of **2c**.Zn^{2+} in DMF/H_2O (7:3, v/v) solvent system under: (A) acidic and (B) basic conditions.

References

1. J. N. Demas and G. A. Crosby, J. Phys. Chem., 1971, 75, 991.